



ARL-TR-9389 • JAN 2022



3D Printing High Performance Computing (HPC) Simulation Results

by Nicholas Kendall, Ethan Eldridge, David Kleponis, and
Stephen Schraml

Approved for public release: distribution unlimited.

NOTICES

Disclaimers

The findings in this report are not to be construed as an official Department of the Army position unless so designated by other authorized documents.

Citation of manufacturer's or trade names does not constitute an official endorsement or approval of the use thereof.

Destroy this report when it is no longer needed. Do not return it to the originator.



3D Printing High Performance Computing (HPC) Simulation Results

Nicholas Kendall
University of Wyoming

Ethan Eldridge
SURVICE Engineering

David Kleponis and Stephen Schraml
*Weapons and Materials Research Directorate,
DEVCOM Army Research Laboratory*

REPORT DOCUMENTATION PAGE

*Form Approved
OMB No. 0704-0188*

Public reporting burden for this collection of information is estimated to average 1 hour per response, including the time for reviewing instructions, searching existing data sources, gathering and maintaining the data needed, and completing and reviewing the collection information. Send comments regarding this burden estimate or any other aspect of this collection of information, including suggestions for reducing the burden, to Department of Defense, Washington Headquarters Services, Directorate for Information Operations and Reports (0704-0188), 1215 Jefferson Davis Highway, Suite 1204, Arlington, VA 22202-4302. Respondents should be aware that notwithstanding any other provision of law, no person shall be subject to any penalty for failing to comply with a collection of information if it does not display a currently valid OMB control number.

PLEASE DO NOT RETURN YOUR FORM TO THE ABOVE ADDRESS.

1. REPORT DATE (DD-MM-YYYY) January 2022		2. REPORT TYPE Technical Report		3. DATES COVERED (From - To) 1 June 2020 – 27 August 2021	
4. TITLE AND SUBTITLE 3D Printing High Performance Computing (HPC) Simulation Results				5a. CONTRACT NUMBER	
				5b. GRANT NUMBER	
				5c. PROGRAM ELEMENT NUMBER	
6. AUTHOR(S) Nicholas Kendall, Ethan Eldridge, David Kleponis, and Stephen Schraml				5d. PROJECT NUMBER	
				5e. TASK NUMBER	
				5f. WORK UNIT NUMBER	
7. PERFORMING ORGANIZATION NAME(S) AND ADDRESS(ES) DEVCOM Army Research Laboratory ATTN: FCDD-RLW-TD Aberdeen Proving Ground, MD 21005				8. PERFORMING ORGANIZATION REPORT NUMBER ARL-TR-9389	
9. SPONSORING/MONITORING AGENCY NAME(S) AND ADDRESS(ES) High Performance Computing Modernization Program Office 7701 Telegraph Rd Alexandria, VA 22315				10. SPONSOR/MONITOR'S ACRONYM(S) HPCMP	
				11. SPONSOR/MONITOR'S REPORT NUMBER(S)	
12. DISTRIBUTION/AVAILABILITY STATEMENT Approved for public release: distribution unlimited.					
13. SUPPLEMENTARY NOTES					
14. ABSTRACT This report presents the feasibility and the methods used to 3D print high performance computing (HPC) simulation results of the formation of shaped charge jets (SCJs) and penetration into armor. The 3D simulations were conducted using computing resources from the US Department of Defense (DOD) HPC Modernization Program, and the Fused Deposition Modeling printer used was the Ultimaker S3. The conversion of 3D HPC simulation results for use with additive manufacturing is presented and shown as a new tool for DOD researchers to visualize, analyze, and compare HPC simulations of SCJ formation and penetration to experimental results.					
15. SUBJECT TERMS additive manufacturing, 3D printing, shaped charge jet, SCJ, rolled homogeneous armor, RHA, fused deposition modeling, FDM, penetration, high performance computing, HPC, simulation, CTH					
16. SECURITY CLASSIFICATION OF:			17. LIMITATION OF ABSTRACT UU	18. NUMBER OF PAGES 22	19a. NAME OF RESPONSIBLE PERSON Ethan Eldridge
a. REPORT Unclassified	b. ABSTRACT Unclassified	c. THIS PAGE Unclassified			19b. TELEPHONE NUMBER (Include area code) (410) 306-4948

Standard Form 298 (Rev. 8/98)
Prescribed by ANSI Std. Z39.18

Contents

List of Figures	iv
Acknowledgments	v
1. Introduction	1
2. Methods and Procedures	1
2.1 The Additive Manufacturing Process	1
2.2 Printing the Shaped Charge Pre-Detonation	2
2.3 Formation of the Jet	5
2.4 Non-Manifold Errors and Penetration into Target Blocks	8
3. Conclusions	11
4. References	13
List of Symbols, Abbreviations, and Acronyms	14
Distribution List	15

List of Figures

Fig. 1	SCJ simulation setup.....	3
Fig. 2	Close-up view of warhead	3
Fig. 3	Simulation of the SCJ formation.....	3
Fig. 4	Components of a warhead. Left to right: 3D-printed model of explosive, 3D-printed model of copper liner, and actual copper liner from the warhead	4
Fig. 5	3-D-printed warhead	5
Fig. 6	3D Benchy with PVA	6
Fig. 7	3D Benchy with PVA removed	6
Fig. 8	Jet formation with PVA support	7
Fig. 9	Jet formation with PVA removed	7
Fig. 10	Jet formation at a later timestep with PVA supports and a PLA raft to ensure the print adheres to the print surface	8
Fig. 11	Jet formation at a later timestep with PVA and PLA raft removed	8
Fig. 12	3D printed target block with unwanted horizontal bands	9
Fig. 13	STL file of target block.....	10
Fig. 14	g-code of target block, oriented vertically. The unwanted bands can be seen in two places along the Z-axis of this model	10
Fig. 15	g-code of target block, oriented face down. 3D printing was performed in this orientation, solving the unwanted horizontal bands issue.....	11

Acknowledgments

The authors thank the DOD High Performance Computing Modernization Program (HPCMP) for the computing resources, the HPCMP Internship Program for sponsoring the primary author as an intern, and the DEVCOM ARL DOD Supercomputing Resource Center and DEVCOM ARL's Multi-Threat Armor Branch for co-hosting the primary author's internship.

1. Introduction

The US Army Combat Capabilities Development Command Army Research Laboratory's Multi-Threat Armor Branch (MTAB) conducts research into armor technologies with a focus on shaped charge jet (SCJ) defeat. These high-velocity penetrators are formed by harnessing and directing the energy from explosives into a copper liner that forms a jet that can penetrate large sections of armor. To analyze these multi-material, large-deformation, strong shock-wave events, the use of solid mechanics codes in computational simulations has been critical to the MTAB research and development.

Through the use of US Department of Defense (DOD) High Performance Computing (HPC) Modernization Program resources, MTAB researchers can use these solid mechanics codes to generate 2D and 3D visual output of the high-velocity events that occur during the formation and penetration of an SCJ. While the use of these visual results can be beneficial when solely viewed on a computer monitor, certain aspects such as scale, the ability to easily compare simulation results with physical experiments, and showcasing what happens during the formation of an SCJ are sometimes more difficult to convey. Additionally, obtaining a 3D physical representation of the warhead formation and penetration event is not possible in experiment. These factors, along with the cost of only performing physical experiments, are strong incentives for exploiting the use of additive manufacturing (AM; also called "3D printing") in conjunction with computational simulations.

2. Methods and Procedures

2.1 The Additive Manufacturing Process

To use an AM process, one must take the results from a 3D simulation and extract the necessary data to generate a geometric file. The most common, and the format used in this study, is called a "Stereo Lithography" file. It has also been called "Standard Triangle Language" or "Standard Tessellation Language" and denoted as an ".stl" (STL) file. The STL file format is used to obtain and encode the surface geometry of a 3D object using a process called tessellation. Through this process the object is covered with geometric shapes (most notably triangles) to take the information from abstract surface points to facets that can be reproduced using AM.

Next in the AM process, the converted geometric file is taken into what is commonly referred to as a "slicer" program. This program takes the encoded geometric file and "slices" the 3D object into layers of a specified thickness, which

results in a geometry-code (g-code) file. The g-code file is what is used to control the filament deposition tool path of the machine. While there are different processes in the AM realm, the focus in this work is on fused deposition modeling (FDM). This is a process where thermoplastics are heated and deposited onto a surface in the pattern specified by the g-code. The model is built layer by layer, usually between 0.05 and 0.4 mm per layer, until the object is recreated. This conversion of the 3D information from the HPC simulations is presented for the Ultimaker S3 3D Printer.

2.2 Printing the Shaped Charge Pre-Detonation

A shaped charge warhead consists of a liner made from a ductile material, typically copper, that is recessed into an explosive, forming a hollow cavity. These liners come in different shapes, materials, and sizes; however, the ones used in this study were all simulated as conical liners made from copper. Using copper allows a long, thin, high-velocity stretching penetrator called a jet to form from the detonating explosive that can efficiently penetrate armor.

Figure 1 shows the setup for a CTH (a shock physics code developed by Sandia National Laboratories) shaped charge simulation. The pink and yellow object on the left make up the shaped charge warhead consisting of the explosive (pink) and a copper liner (yellow). The alternating shades of gray blocks are rolled homogeneous armor (RHA) steel target blocks. When the explosive detonates, a shockwave propagates up through the copper liner causing the copper liner to invert from the cone apex forward to the base within the hollow cavity, forming a high velocity jet that penetrates the RHA plates. A close-up of the warhead is seen in Fig. 2, and the jet formation is shown in Fig. 3. The jet is colored by axial velocity bands ranging from 8.0 to 9.2 km/s at the tip (black) to 0 to 1 km/s at the base (yellow).

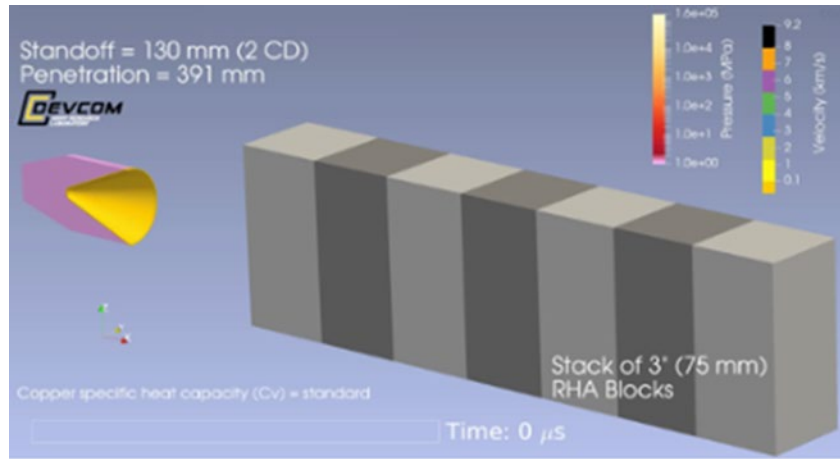


Fig. 1 SCJ simulation setup

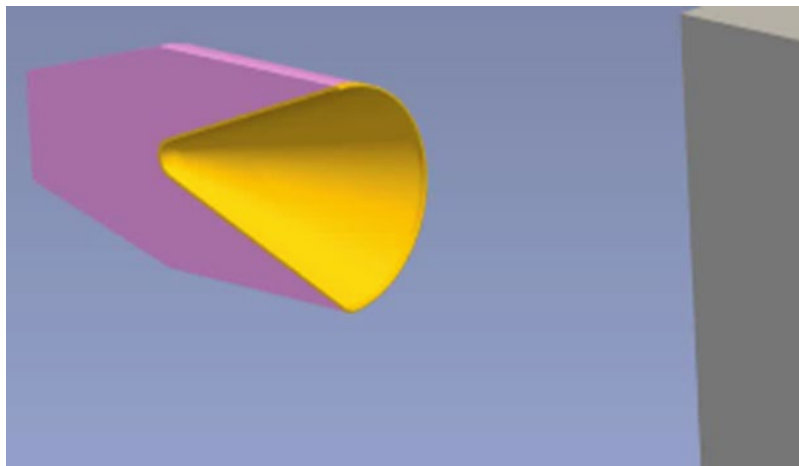


Fig. 2 Close-up view of warhead

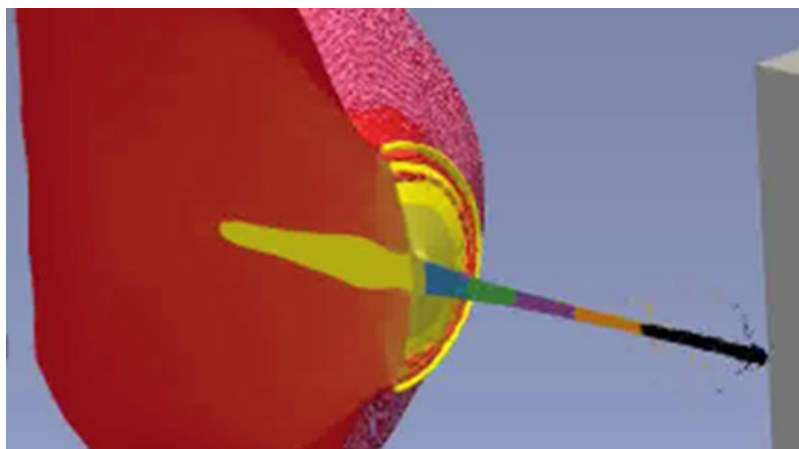


Fig. 3 Simulation of the SCJ formation

The software tool used to visualize the simulation was Paraview version 5.8.0. Using this software, the initial model of the warhead was taken before it was detonated. The liner and explosive were isolated, and the data had a filter applied to extract the surface. This allowed for a triangulation filter to be applied to the extracted surface of the model. These two steps were essential because the FDM printer requires the surface geometry of a 3D object to be made out of facets. Since the two models were encoded with triangular surface features, the models could be exported out of Paraview as an STL file. These STL files were imported into the Ultimaker Cura slicer program for the Ultimaker S3 3D printer. Once the g-code was produced, the models were 3D printed as shown in Fig. 4 along with a copper liner from an actual warhead. Figure 5 shows the assembled 3D printed components of the warhead.

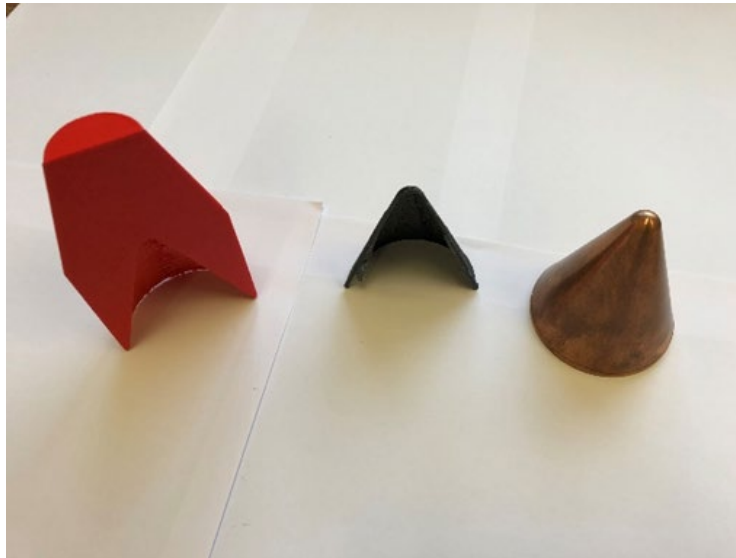


Fig. 4 Components of a warhead. Left to right: 3D-printed model of explosive, 3D-printed model of copper liner, and actual copper liner from the warhead



Fig. 5 3-D-printed warhead

2.3 Formation of the Jet

Large deformations in the liner occur during the jet formation process. This results in difficulties obtaining a usable 3D model for printing. The large deformation of the liner creates overhangs, small surface features, and floating entities within the 3D model. Since FDM printers use a thermoplastic filament that is extruded layer by layer, they cannot replicate overhangs or suspended particles without support structures.

The Ultimaker S3 3D Printer used for this work can use two different materials during the 3D printing process. The first is polylactic acid (PLA) plastic, the most common plastic used in desktop 3D printing. It is made from renewable resources such as sugar cane or corn starch and is popular because it prints at a low temperature. This also allows PLA to be a low-warp material, so there is minimal material contraction when it cools, meaning it is very dimensionally accurate and stable. The second material is polyvinyl alcohol (PVA), which is soluble in water, making it very useful as a support material. Using PVA to print supports enables more-complicated geometries and overhangs to be created. It also makes it easy to remove the support material after the model is printed since it can be placed in water to dissolve the PVA, leaving behind the solidified PLA model.

Experiments were conducted with PVA to evaluate its reliability. This was done by printing several 3D Benchy models (CreativeTools 2015) using PVA support material. Although the 3D Benchy model is designed to print without support materials, it was a convenient standard model to use to print PVA and PLA for evaluation. The resulting Benchy prints were then used to determine the length of time the PVA takes to fully dissolve. Figure 6 is the Benchy model printed with

PVA supports, and Fig. 7 is the same Benchy after the PVA was removed. On average, it took about 24 h for the PVA to dissolve in room temperature water.

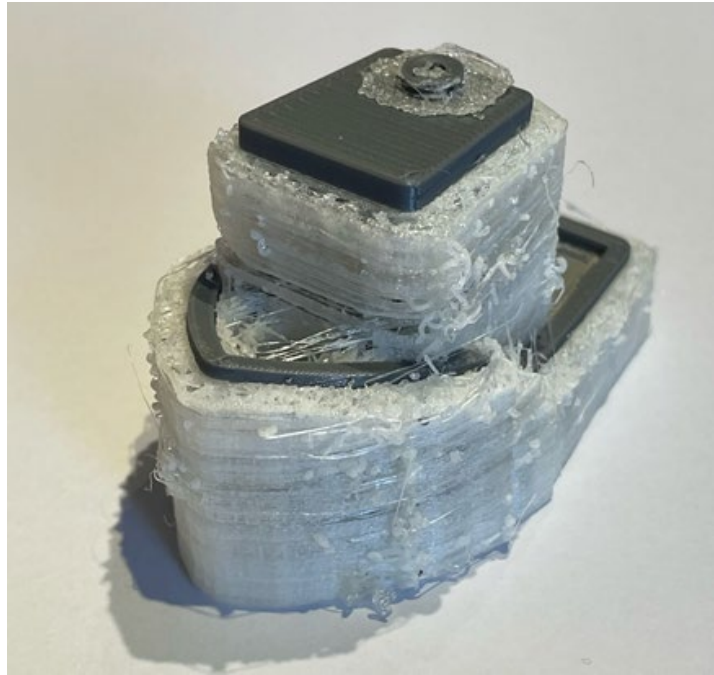


Fig. 6 3D Benchy with PVA

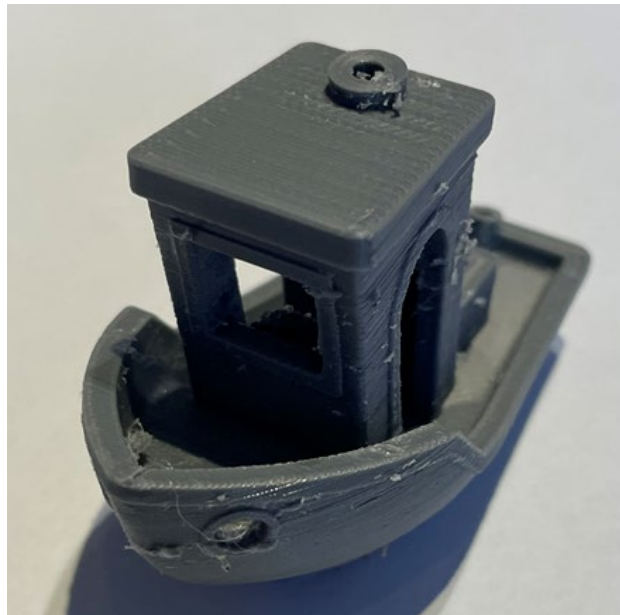


Fig. 7 3D Benchy with PVA removed

After ensuring the soluble supports would dissolve reliably, the SCJ was printed in half symmetry during its formation. Figure 8 shows the 3D printed SCJ in half

symmetry along with the PVA supports, while Fig. 9 shows the same SCJ but with the PVA supports removed. Since the jet formation at a later timestamp was more delicate (Fig. 10), addition of a PLA raft was required to increase the surface area of the print to ensure the print adhered to the print surface. Figure 11 shows the same SCJ with the PVA supports removed. As seen with the large amount of support material around the portion of the cone that has not yet collapsed, it would have been impossible to print and remove the support material without using PVA. The PVA worked reliably as a support system for these 3D prints, and a method for printing SCJ formation from 3D HPC simulations was demonstrated.



Fig. 8 Jet formation with PVA support



Fig. 9 Jet formation with PVA removed



Fig. 10 Jet formation at a later timestep with PVA supports and a PLA raft to ensure the print adheres to the print surface

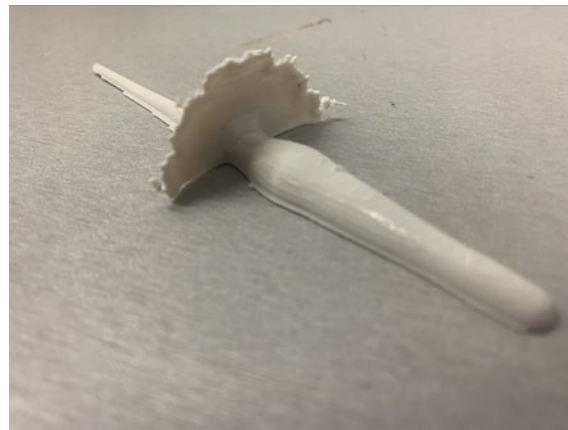


Fig. 11 Jet formation at a later timestep with PVA and PLA raft removed

2.4 Non-Manifold Errors and Penetration into Target Blocks

Non-manifold errors arose while generating the STL and geometry files from the RHA target block penetration and jet formation. Non-manifold geometries are defined as edges that are shared by more than two faces, that in this case are errors that likely arise during the geometry mesh creation. These non-manifold errors are commonly unnecessary structures inside a 3D object or shared vertices and/or faces that produce invalid geometries for 3D printing. Using Autodesk Meshmixer and Meshlab, these errors can be solved by manually removing invalid geometries or combining the shared vertices and faces.

While this approach corrected most errors that occurred, the RHA target blocks proved to be more challenging than expected. This may be an artifact of the meshing process in the simulation. In Fig. 12 horizontal bands of empty space were seen at regular intervals through the target block. This phenomenon is thought to

be caused by non-manifold surfaces in the 3D model that could be related to the variable sizes of the computational mesh used in the target block of the simulation as shown via red lines in Fig. 13. One theory is the slicer sees the non-manifold edges, the affected layers are deleted from the final print file, and support material is put in its place instead. A temporary fix through a process in Meshlab proved to resolve most of the issues in the g-code development. This included removing isolated floating pieces from the 3D model in combination with using built-in cleaning and repairing filters to remove duplicate faces, remove duplicate vertices, merge close vertices, and remove isolated folded faces by edge flip. If the g-code still came out with missing or non-manifold portions, changing the orientation of the model on the build plate would usually solve the irregularities, as shown in Figs. 14 and 15. While additional work is required to understand or fully overcome this irregularity, an initial method for printing a 3D penetration channel from 3D HPC simulations was demonstrated.



Fig. 12 3D printed target block with unwanted horizontal bands

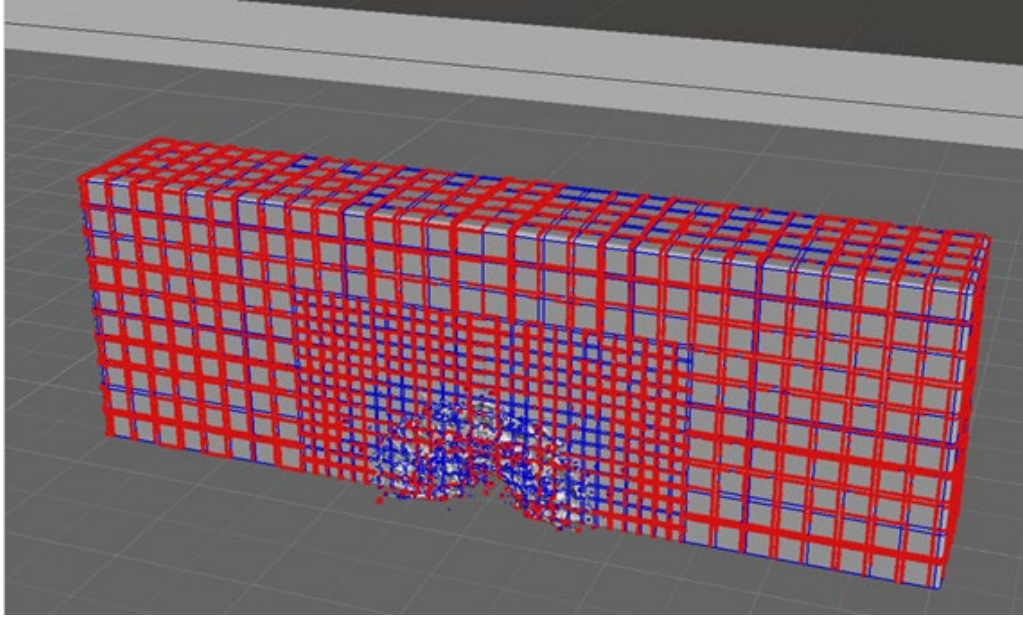


Fig. 13 STL file of target block

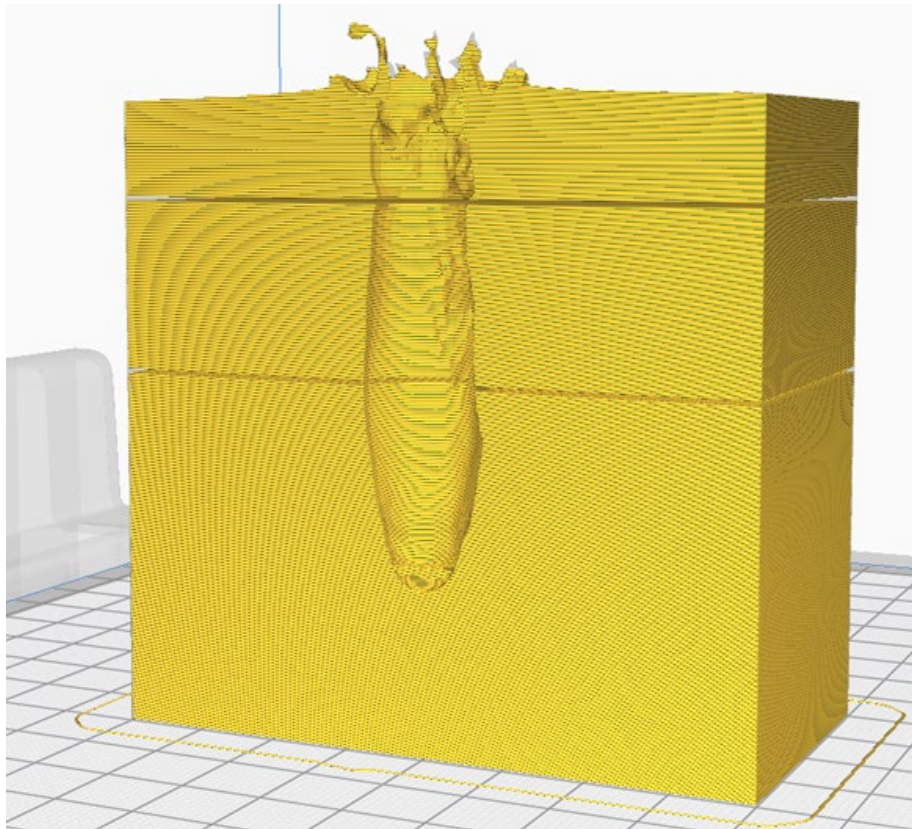


Fig. 14 g-code of target block, oriented vertically. The unwanted bands can be seen in two places along the Z-axis of this model

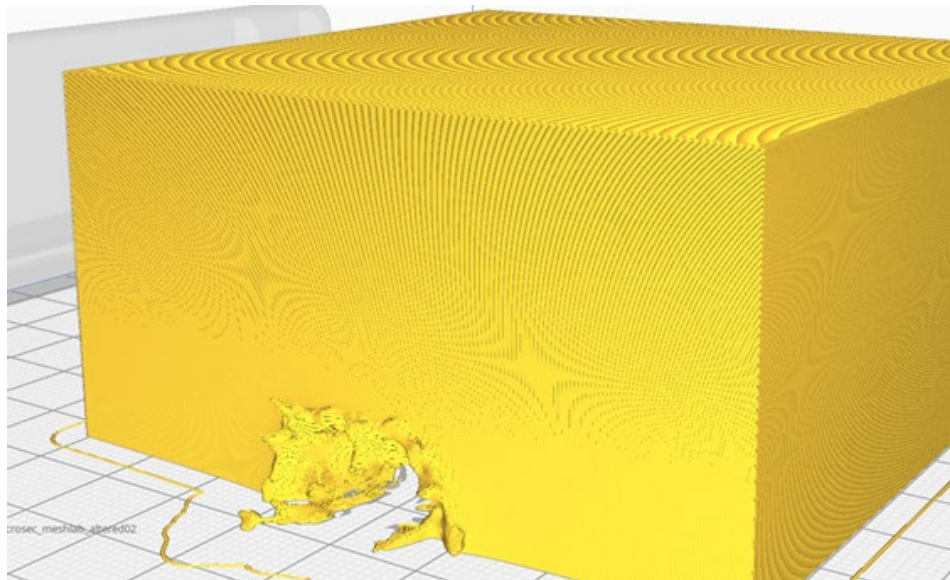


Fig. 15 g-code of target block, oriented face down. 3D printing was performed in this orientation, solving the unwanted horizontal bands issue

3. Conclusions

A method for using AM to 3D print results from 3D HPC simulations was demonstrated. This new capability provides researchers with a new tool for analyzing and observing complex phenomena through 3D physical representations of those simulations, as seen in the present case of SCJ warhead formation and RHA penetration. This new tool provides the ability to generate 3D physical representations of complex ballistics at event times that are impossible to obtain through experimentation. It also provides a tool that can be used for physical comparison of final experimental results to simulation results. An interesting byproduct of the capability is that a new teaching and marketing tool now exists. 3D physical representations are easier to relate to the uninitiated. Tactile objects provide more context and a better understanding of scale, and can be much more interesting than pictures on a monitor or on a page.

The use of PVA provided the capability to remove supports without the risk of damaging fragile geometries by eliminating the need for tedious post-processing such as cutting or sanding. However, the PVA filament is many times more expensive than PLA filament and requires a dual-extruder 3D printer, but it is well worth the increase in cost for the resulting print capability and quality. Dual extrusion can also be challenging at times because it requires additional calibration to align the print heads and to adjust the print temperatures correctly. The resulting use of PVA enabled challenging geometries to be printed that would not have been possible with only using PLA or with a single-extruder printer.

The exporting process and complexity of generating the required g-code seems to vary between the SCJ and the target blocks. While the SCJ exports cleanly to the slicer, the target blocks exhibited multiple manifold errors. These manifold errors meant that the model was either invalid or undefined at specific locations, causing import/export issues in the slicer and subsequent g-code. Some of these issues go on to cause printing errors that are not fully understood. While additional work is required to understand and overcome these irregularities, an initial method for printing a 3D SCJ and its penetration channel was demonstrated.

3D printing of HPC simulations provides a new range of opportunities for DOD researchers to use HPC simulations. Currently, researchers use solid mechanics codes to generate 2D and 3D visual output of their HPC simulations. However, the ability to compare the simulation results with physical experiments is limited to numerical values and non-physical material plots. The use of 3D printing in conjunction with computational simulations not only minimizes the number of costly physical experiments, it provides a 3D physical representation of the warhead formation and penetration event not possible in experiments and provides the ability to directly compare physical simulation results with physical experimental results.

4. References

CreativeTools. #3DBenchy – The jolly 3D printing torture-test by CreativeTools.se; 2015 Apr 09 [accessed 20 May 2021]. Makerbot: Thingiverse. www.thingiverse.com/thing:763622.

List of Symbols, Abbreviations, and Acronyms

2D	two-dimensional
3D	three-dimensional
AM	additive manufacturing
DOD	Department of Defense
FDM	fused deposition modeling
g-code	geometry code
HPC	high performance computing
HPCMP	High Performance Computing Modernization Program
MTAB	Multi-Threat Armor Branch
PLA	polylactic acid
PVA	polyvinyl alcohol
RHA	rolled homogeneous armor
SCJ	shaped charge jet
STL	Stereo Lithography or Standard Triangle Language or Standard Tessellation Language

1 DEFENSE TECHNICAL
(PDF) INFORMATION CTR
DTIC OCA

1 DEVCOM ARL
(PDF) FCDD RLD DCI
TECH LIB

3 DEVCOM ARL
(PDF) FCDD RLW TD
E ELDRIDGE
D KLEPONIS
S SCHRAML